B-T-3653

COBRA-IE EVALUATION BY SIMULATION OF THE NUPEC BWR FULL-SIZE FINE-MESH BUNDLE TESTS (BFBT)

C. J. Burns and D. L. Aumiller

BECHTEL BETTIS, INC. WEST MIFFLIN, PENNSYLVANIA 15122-0079

COBRA-IE Evaluation by Simulation of the NUPEC BWR Full-Size Fine-Mesh Bundle Tests (BFBT)

Christopher J. Burns
David L. Aumiller
Bechtel Bettis Inc.
P.O. Box 79
West Mifflin, PA 15122-0079, USA

The COBRA-IE computer code is a thermal-hydraulic subchannel analysis program capable of simulating phenomena present in both PWRs and BWRs. As part of ongoing COBRA-IE assessment efforts, the code has been evaluated against experimental data from the NUPEC BWR Full-Size Fine-Mesh Bundle Tests (BFBT). The BFBT experiments utilized an 8x8 rod bundle to simulate BWR operating conditions and power profiles, providing an excellent database for investigation of the capabilities of the code. Benchmarks performed included steady-state and transient void distribution, single-phase and two-phase pressure drop, and steady-state and transient critical power measurements. COBRA-IE effectively captured the trends seen in the experimental data with acceptable prediction error. Future sensitivity studies are planned to investigate the effects of enabling and/or modifying optional code models dealing with void drift, turbulent mixing, rewetting, and CHF.

I. Introduction

COBRA-IE is being developed as a thermal-hydraulic subchannel analysis code. Based on COBRA-TF (Coolant Boiling in Rod Arrays - Two Fluid), the Integrated Environment (IE) version resolves underlying deficiencies in the program, fixes code errors, and adds new features to create a useful analysis tool.

The NUPEC BWR Full-Size Fine-Mesh Bundle Tests (BFBT) (Reference 1) effectively simulate the steady-state and transient behavior of boiling water reactors. A wide variety of experiments have been performed, focusing on pressure drop, void distribution, and critical power measurements. These tests provide an excellent database for assessing the accuracy of many of the features of COBRA-IE.

II. Experimental Facility

1. Test Section

The BFBT test section, shown in Figure 1 (Reference 1), consists of an outer pressure vessel, inlet and outlet nozzles, and fuel rods with a 3708mm heated length. An inner square channel box contains an 8x8 array of simulated 12.3mm diameter fuel rods and one large (34.0 mm diameter) or two small (15.0 mm diameter) water rods. Some configurations also contain unheated rods to create large transverse void distribution gradients. Figure 2 shows the different configurations used in the BFBT experiments. The simulated fuel rods are indirectly electrically heated to provide simulation of actual nuclear reactor power profiles. To support the rods, seven spacers are installed in the bundle at the axial locations shown in Figure 3. The bundle with one large water rod utilizes ferrule-type spacers, while the bundles with two small water rods contain grid-type spacers as shown in Figure 4.

2. Instrumentation

The BFBT test section is outfitted with all the instrumentation required to measure pressure drop, void fraction, and critical power.

The local void fraction is measured at four axial locations as shown in Figure 5. At three elevations within the bundle, X-ray densitometers are installed to provide line-averaged void fractions by emitting a beam between the rods into a detector. The X-ray tubes and detectors are moved horizontally to cover the entire bundle width. Above the top of the heated bundle, a rotating X-ray CT scanner is installed to measure the cross-sectional void fraction.

The X-ray CT scanner has a resolution of 3mm, allowing fine-mesh void distribution maps to be created.

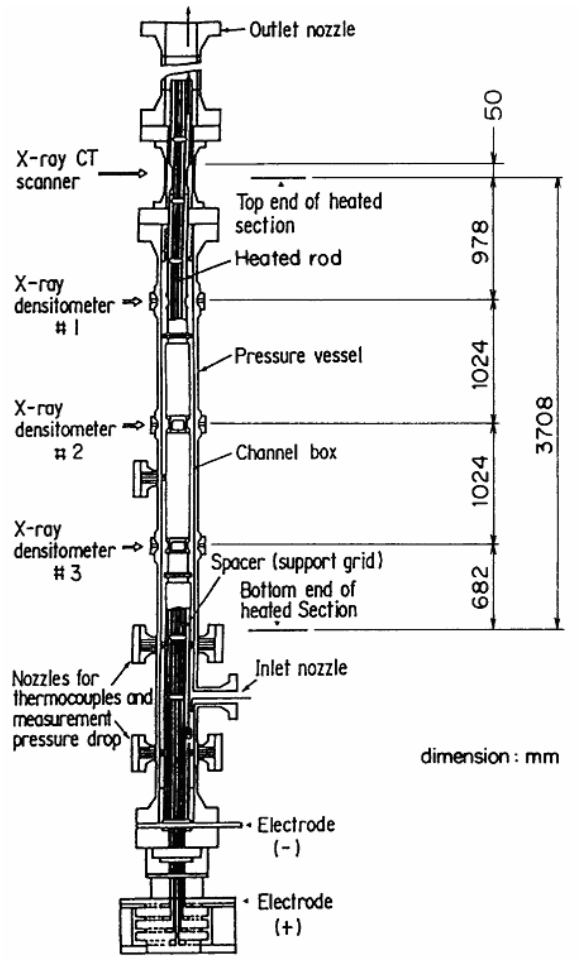

Figure 1. Test Section

Pressure drop is measured using taps installed at nine axial locations, with the shortest covering 210mm and the longest spanning the entire heated length of the bundle. Single-phase and two-phase pressure drop data was obtained for a variety of flow conditions and power shapes.

Critical power, the minimum power at which critical heat flux (CHF) occurs in the test section, is measured with thermocouples installed circumferentially in the cladding of the hottest rods. The thermocouples are axially located 6mm upstream of each of the top 2, 3, or 4 spacers (depending on the configuration),

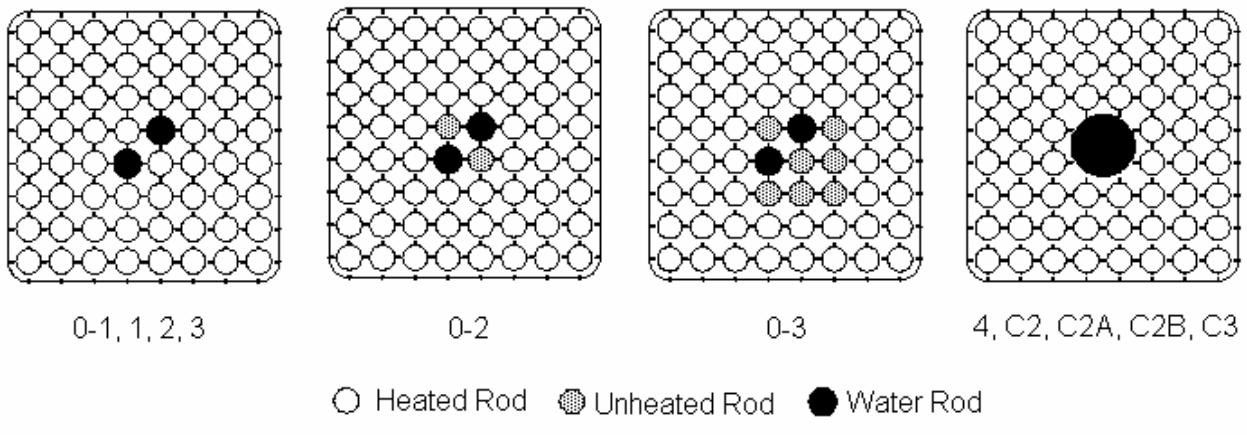

Figure 2. Different configurations of the BFBT test section

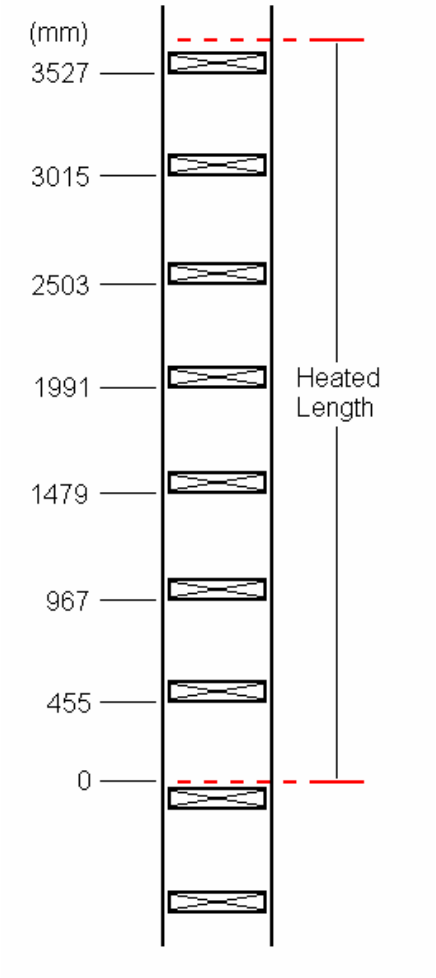

Figure 3. Spacer Locations

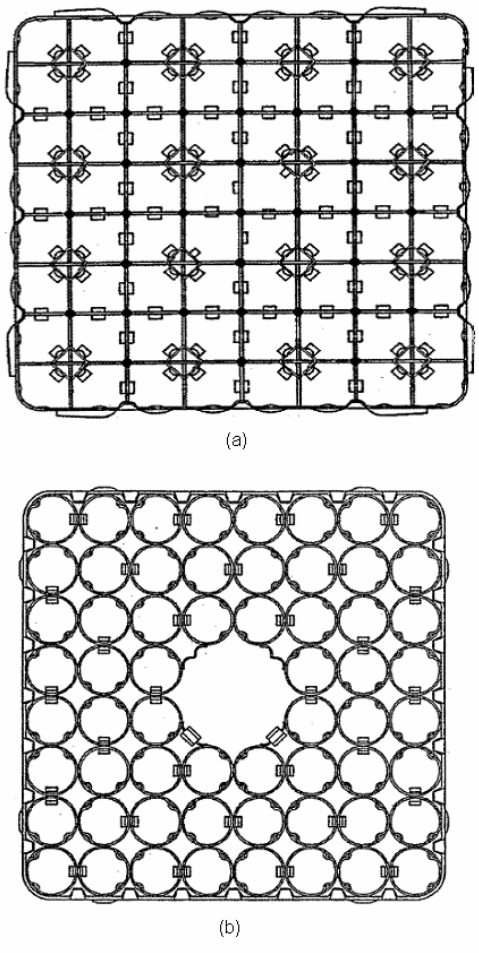

Figure 4. Grid (a) and Ferrule (b) Spacers

where dryout is most likely to occur. Critical power is indicated when the peak rod surface temperature becomes 14°C higher than the steady-state temperature before dryout occurs.

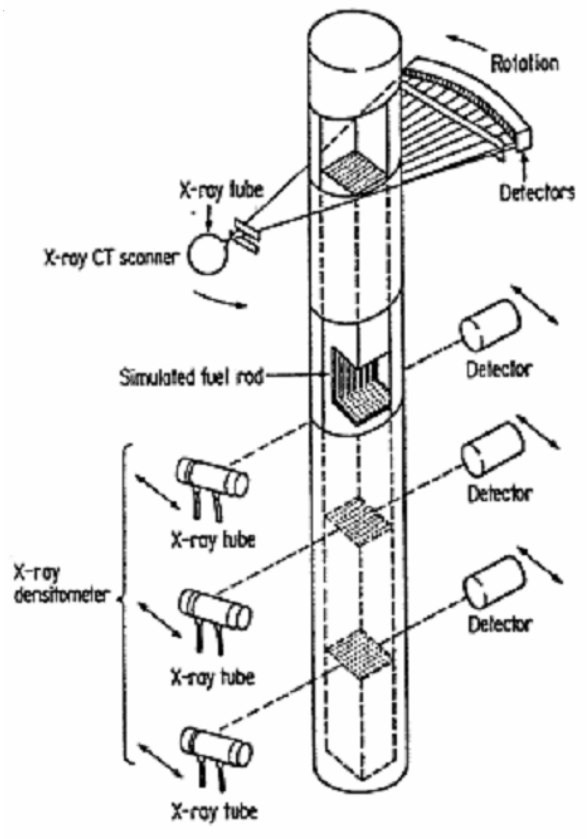

Figure 5. Void Measurement System

III. COBRA-IE Computer Code

COBRA-IE is another in the series of the COBRA subchannel analysis computer programs which were originally developed by Pacific Northwest Laboratories (PNL). The largest difference between COBRA-IE and previous versions of COBRA is that COBRA-IE can be used with the PVMEXEC program (Reference 2). PVMEXEC is a program that provides a computing infrastructure in which various computer programs such as COBRA-IE, RELAP5-3D or MELCOR can be coupled together to provide an integrated analysis tool. When used in the PVMEXEC system, COBRA-IE is most frequently coupled to RELAP5-3D (Reference 3) such that behavior of the reactor loops, pumps, steam generators, etc. can be directly included in the COBRA analyses. The hydraulic coupling of COBRA with RELAP5-3D uses a numerically stable, semi-implicit coupling algorithm (Reference 4). COBRA-IE has been coupled to the point-kinetics algorithm in RELAP5-3D to provide the proper response of thermal-hydraulic conditions on reactor power. To denote the capability of this version of COBRA to operate in the PVMEXEC integrated code system, it has been renamed as COBRA-IE where IE stands for **I**ntegrated **E**nvironment.

COBRA-IE is based on a version of COBRA-TF from the Pennsylvania State University (PSU). Starting with a version of COBRA-TF that had replaced the old common-block memory structure and had an incomplete implementation of the non-condensable gas field, PSU developed a version of COBRA for reflood in small-hydraulic geometries. Reference 5 contains a comprehensive description of this version of the COBRA-TF program including the conservation equations, interfacial heat transfer and heat transfer models.

The transition from COBRA-TF to COBRA-IE involved the development of many new features and the correction of deficiencies in the donor code. In addition to the coupling work, the following is a partial list of the new features that have been added to the COBRA-IE program: a sparse-matrix direct solver, new boundary conditions, a new correlation for T_{min} and a model for the effect of non-condensables on condensation.

Most of the deficiencies that have been corrected in the donor code were related to the incomplete implementation of the non-condensable gas field. To address these issues, the interfacial heat/mass transfer package and the linearization of the

temporal derivative were completely rewritten.

As a result of the added features and error corrections, the robustness and capability of COBRA-IE have both been significantly enhanced. The combination of RELAP5-3D and COBRA-IE creates a very powerful tool for analyzing transients such as Large-Break Loss-of-Coolant-Accidents (LB-LOCA's).

IV. Experimental Method and Test Conditions

1. Void Distribution Benchmark

The BFBT experiments were divided into two phases; the first of which was a void distribution benchmark utilizing seven of the configurations (0-1, 0-2, 0-3, 1, 2, 3, and 4) illustrated in Figure 2. Steady-state and transient experiments were performed, with data provided on a per-subchannel basis at the four axial sampling locations shown in Figure 5.

The steady-state subchannel void distributions were measured by holding flow conditions constant for 60 seconds while sampling with the X-ray densitometers and rotating CT scanner. Nearly 400 nonunique steady-state test cases were run, fifteen of which have been designated as unique representative exercise cases. The same flowrate was used for each test, with the exit quality varied with bundle power. Table 1 outlines the experimental conditions for the steady-state void distribution benchmark.

Table 1. Steady-State Void Distribution Test Conditions

Configurations	0-1, 0-2, 0-3, 1, 2, 3, 4
Pressure (MPa)	7.2
Flowrate (t/h)	55
Inlet Subcooling (kJ/kg)	50.2
Exit Quality (%)	5, 12, 25

In addition to the steady-state test cases, two transients were simulated by varying bundle power and coolant flow: a turbine trip without bypass and a recirculation pump trip. Each of these transients lasted approximately 60 seconds, with void fraction measurements taken every 0.02 seconds. The experiments were repeated nine times each while moving the X-ray densitometer horizontally to allow sampling of each channel. The CT scanner measurements were averaged over the nine runs. Table 2 outlines the experimental conditions for the transient void distribution benchmark.

Table 2. Transient Void Distribution Test Conditions

	Configuration	4
Initial Conditions	Pressure (MPa)	7.2
	Power (MW)	4.5
	Flowrate (t/h)	55
	Inlet T (°C)	279

2. Pressure Drop Benchmark

Phase two consisted of pressure drop and critical power measurement benchmarks. The 36 isothermal single-phase and 33 heated two-phase pressure drop experiments were performed using Configurations C2 and C2A respectively, as shown in Figure 2. The range of test conditions used in the pressure drop experiments is given in Table 3.

Table 3. Pressure Drop Test Conditions

Single-Phase	Configuration	C2
	Pressure (MPa)	0.1, 0.98, 7.2
	Flowrate (t/h)	10, 15, 20, 25, 30, 35, 40, 45, 55, 60, 65, 70
	Inlet Temperature	285°C

Table 3. (cont) Pressure Drop Test Conditions

Two-Phase	Configuration	C2A
	Pressure (MPa)	7.2, 8.6
	Flowrate (t/h)	20, 45, 55, 70
	Inlet Subcooling (kJ/kg)	50.2
	Exit Quality (%)	7, 10, 15, 20, 25

3. Critical Power Benchmark

The critical power benchmark portion of Phase 2 was divided into steady-state and transient experiments using Configurations C2A (cosine power profile, high transverse peaking), C2B (cosine profile, low transverse peaking), and C3 (inlet-peak profile, high transverse peaking) from Figure 2. The steady-state critical power measurements were taken by gradually increasing the bundle power until a surface thermocouple indicated a rapid temperature rise of 14°C. Of the 151 nonunique steady-state experiments performed, 44 have been chosen as unique representative exercise cases. Table 4 shows the test conditions used for the steady-state critical power benchmark.

Table 4. Steady-State Critical Power Test Conditions

Configurations	C2A, C2B, C3
Pressure (MPa)	5.5, 7.2, 8.6
Flowrate (t/h)	20, 30, 45, 55, 60, 65
Inlet Subcooling (kJ/kg)	25, 50, 84, 104, 126

As with the void distribution benchmark, the transient critical power experiments simulated a turbine trip without bypass and a recirculation pump trip. Each transient scenario was simulated twice, once with Configuration C2A and once with C3.

Temperatures were recorded every 0.02 seconds using thermocouples mounted to the surfaces of the rods. The simulations continued after critical power was reached, and included rewetting of the rod surfaces. The test conditions used for the transient critical power benchmark are outlined in Table 5.

Table 5. Transient Critical Power Test Conditions

Configurations	C2A, C3
Pressure (MPa)	7.2
Power (MW)	6.2 - 8.5
Flowrate (t/h)	45
Inlet Enthalpy (kJ/kg)	1217 - 1227

V. COBRA Input Model

To assess the capabilities of the code, COBRA-IE input was constructed to model each of the BFBT configurations. The geometry and power profiles used in the experiments allow for diagonal half-bundle symmetry to be used, as shown in Figure 6. Inlet boundary conditions were specified for total mass flow and enthalpy, with an initial estimate of inlet pressure input for fluid property calculations only. At the bundle outlet, the upper plenum pressure was specified. A radial power factor was identified for each rod; axial power factors were used to simulate realistic power shapes by dividing the bundle into 24 discrete axial nodes, each 154.5mm in length.

COBRA-IE allows for some flexibility in modeling by permitting the user to adjust correlational parameters and select various constitutive relations. For purposes of benchmarking, code defaults were primarily used to provide an assessment of baseline performance.

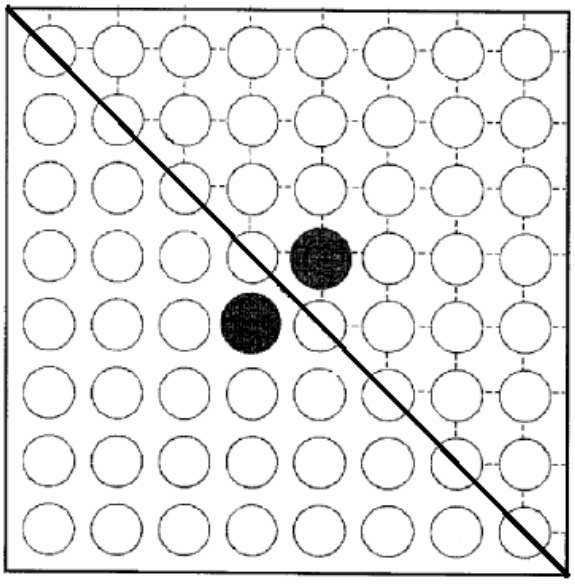

Figure 6. Symmetry Used in COBRA-IE Models

Best estimate input was used exclusively in the COBRA-IE model. No attempt was made to "tune" the input data or calculational parameters to provide better agreement between COBRA-IE calculations and the experimental results.

For pressure drop calculations, Blasius friction factors were used along with spacer loss coefficients provided by the experimenters. For the void distribution calculations, the void drift and turbulent mixing enhancement models were disabled. The well-tested Biasi correlation (Reference 6) was used to calculate critical heat flux (CHF) in the critical power calculations.

The COBRA-IE models were run by first allowing the flow and power to stabilize for 20.0 seconds, then initiating the desired transient or investigating the steady-state parameter in question. All 69 single-phase and two-phase pressure drop cases were modeled. For the void distribution and critical power experiments, only the unique representative exercise cases were modeled.

VI. Analysis Results

1. Void Distribution Benchmark

a. Steady-State

The results of the COBRA-IE steady-state void distribution calculations were compared to values recorded with the X-ray CT scanner mounted above the heated bundle. The X-ray densitometer readings were not included in the comparisons, since the experimenters measured line-averaged void fraction while COBRA-IE calculates area-averaged void fraction.

COBRA-IE calculates void fractions on a per-subchannel basis, allowing for direct comparison between void fractions in specific regions. Figure 7 shows the measured and calculated average exit void fractions, with COBRA-IE slightly overestimating the void fraction in each case. This overall discrepancy is under investigation. Figure 8 illustrates the absolute value of the relative error seen between measured and calculated results averaged over all subchannels, as shown below:

$$E = \frac{1}{n_{subchs}} \sum_{subch's} \left| \frac{\alpha_{meas,subch} - \alpha_{calc,subch}}{\alpha_{meas,subch}} \right|$$

Figure 8 clearly indicates that for all power shapes the calculational accuracy improves as the exit or local quality increases. All cases used the same flowrate, as void distribution was varied with bundle power. Note that the absolute error, while greater for lower qualities, is not excessive. For the higher-quality cases (12% and 25%), most calculated values were within 10% of the measured void fractions, with a maximum error of 14%. Accurate prediction of the higher quality region is more important in BWR calculations, since under normal operating conditions the exit quality is typically greater than 10%.

Void distribution maps have been created for visual comparison to measured

data. The measured and calculated void distribution maps for Configuration 0-3 with 5%, 12%, and 25% exit qualities are shown in Figure 9. This representative figure shows that the subchannel void distributions are accurately predicted by COBRA-IE for the high-quality cases, and that the locations of regions of especially high and low void fraction are well-captured for all three qualities. Activation of the COBRA-IE void drift and/or turbulent mixing enhancement models may further improve the accuracy of the calculation, but these models rely partially on user-defined parameters for which there were no physical bases for input in these cases.

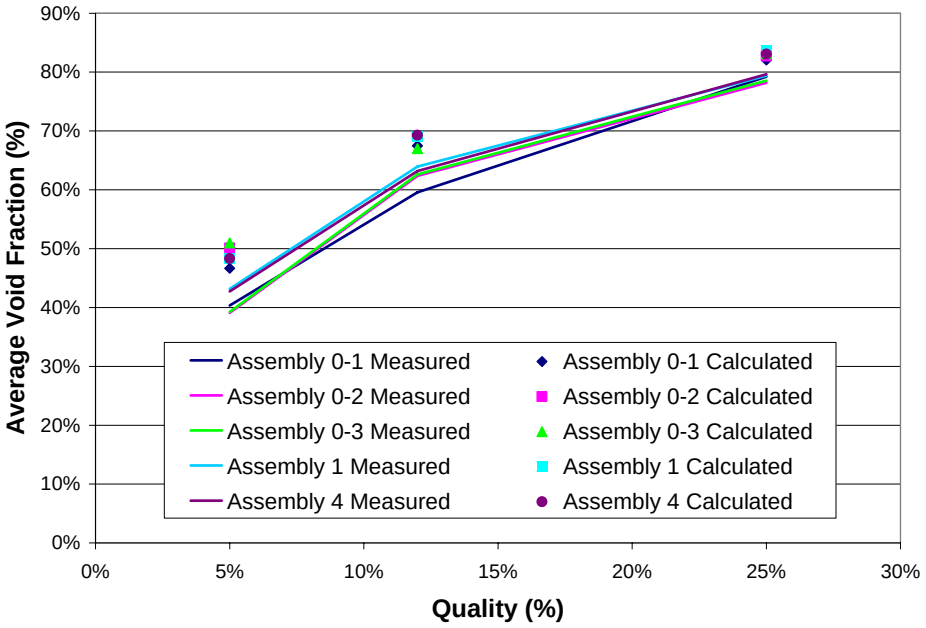

Figure 7. Steady-State Void Distribution Absolute Error

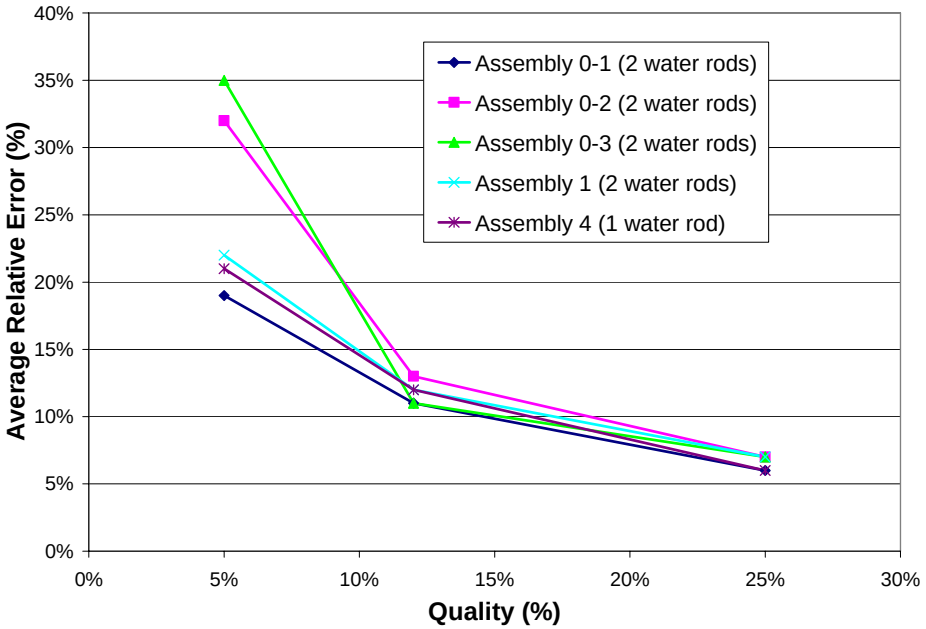

Figure 8. Steady-State Void Distribution Relative Error

b. Transient

COBRA-IE simulations of the turbine trip without bypass and recirculation pump trip transients yielded predictable results when compared to the limited measured data. Figures 10 and 11 show the comparison of calculated and measured area-averaged bundle exit void fraction for the turbine and pump trip cases, respectively. Measured data was only available for the first 32 seconds of the transients. In both cases, the calculated histories follow the trends of the measured data, but overestimate the void fraction by approximately 10%. This discrepancy is currently under investigation.

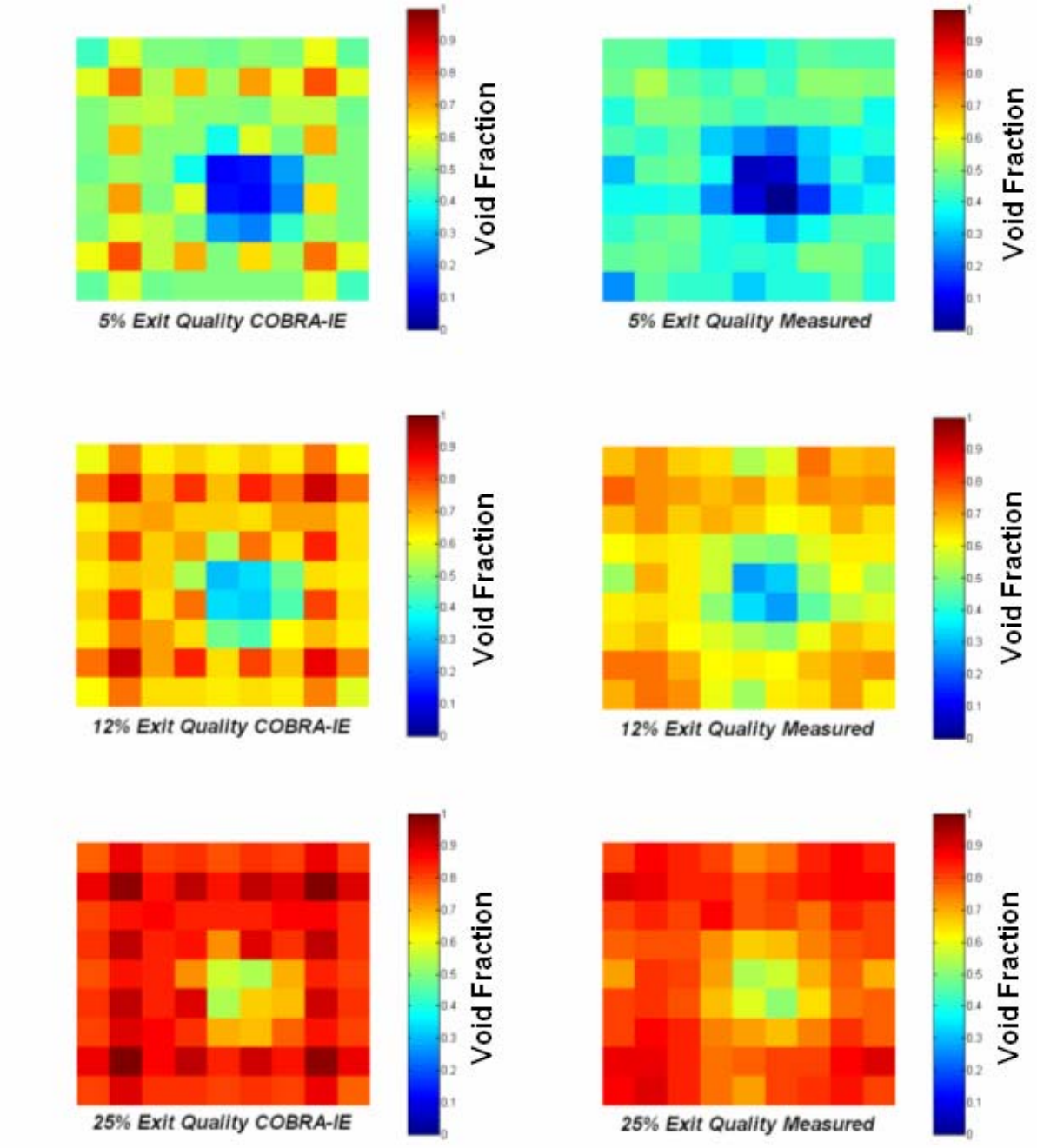

Figure 9. Calculated and Measured Void Distribution Maps for Configuration 0-3

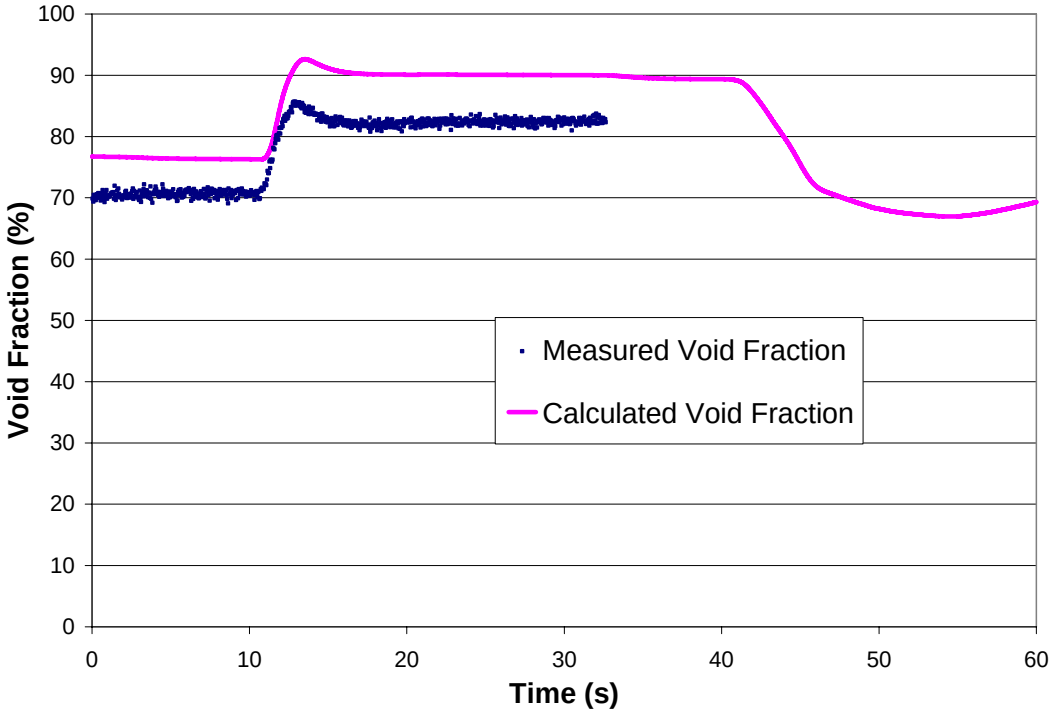

Figure 10. Turbine Trip Exit Void Fraction

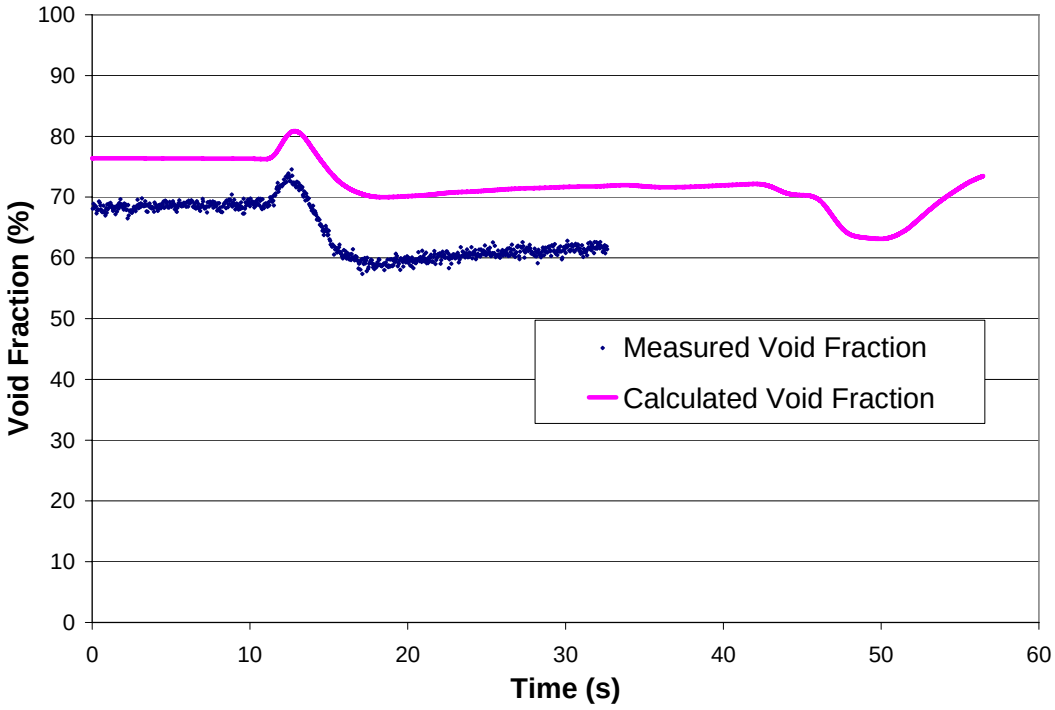

Figure 11. Pump Trip Exit Void Fraction

2. Pressure Drop Benchmark

All of the pressure drop benchmark cases were steady-state, with 36 isothermal single-phase runs and 33 heated two-phase runs. A compilation of all single-phase and two-phase COBRA-IE results and measured data is shown in Figure 12. Excellent agreement is seen between calculated and measured values, indicating that COBRA-IE is capable of accurately performing single-phase and two-phase pressure drop calculations. The average error for the single-phase cases was less than 1%. For the two-phase cases, the average error was 11%. Most of the uncertainty was attributed to low-flow test cases, with less than 4% average error among all other cases.

3. Critical Power Benchmark

a. Steady-State

To determine steady-state critical power using COBRA-IE, multiple calculations were performed while incrementally increasing the bundle power until CHF was indicated. In this manner, a critical power range was obtained between the highest calculated non-CHF power and the lowest calculated CHF power. For the BFBT cases, the resolution of this range was 1% of the experimentally measured critical power. Figure 13 shows the COBRA-IE calculated and measured critical power levels. Good agreement is seen between the calculated and measured values, as the COBRA-IE implementation of the Biasi correlation proves accurate for the BFBT conditions. Parametric trends showing the effect of system pressure and flow on CHF prediction accuracy are shown in Figures 14 and 15, respectively. The underprediction of critical power at lower flows is typical of the Biasi correlation (Reference 7). The average error for the steady-state critical power results was 4.78%, consistent with the published Biasi accuracy of 7.26% (Reference 6).

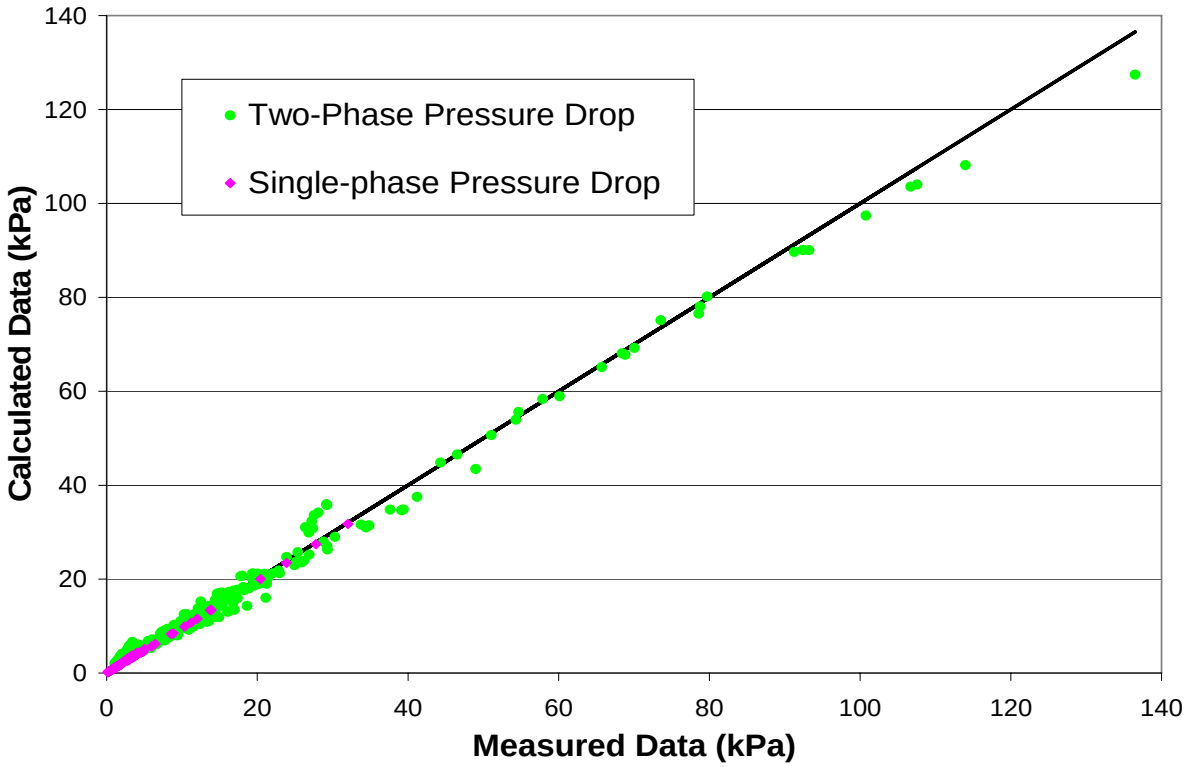

Figure 12. Single-Phase and Two-Phase Pressure Drop Results

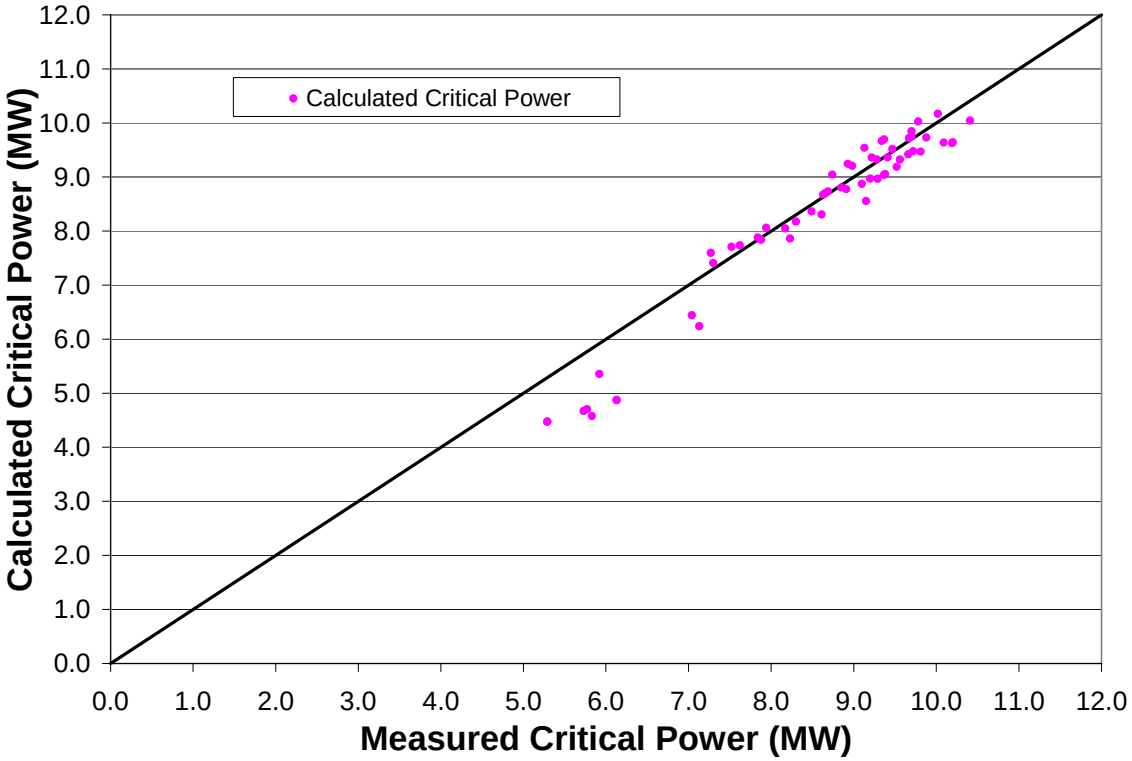

Figure 13. Steady-State Critical Power Results

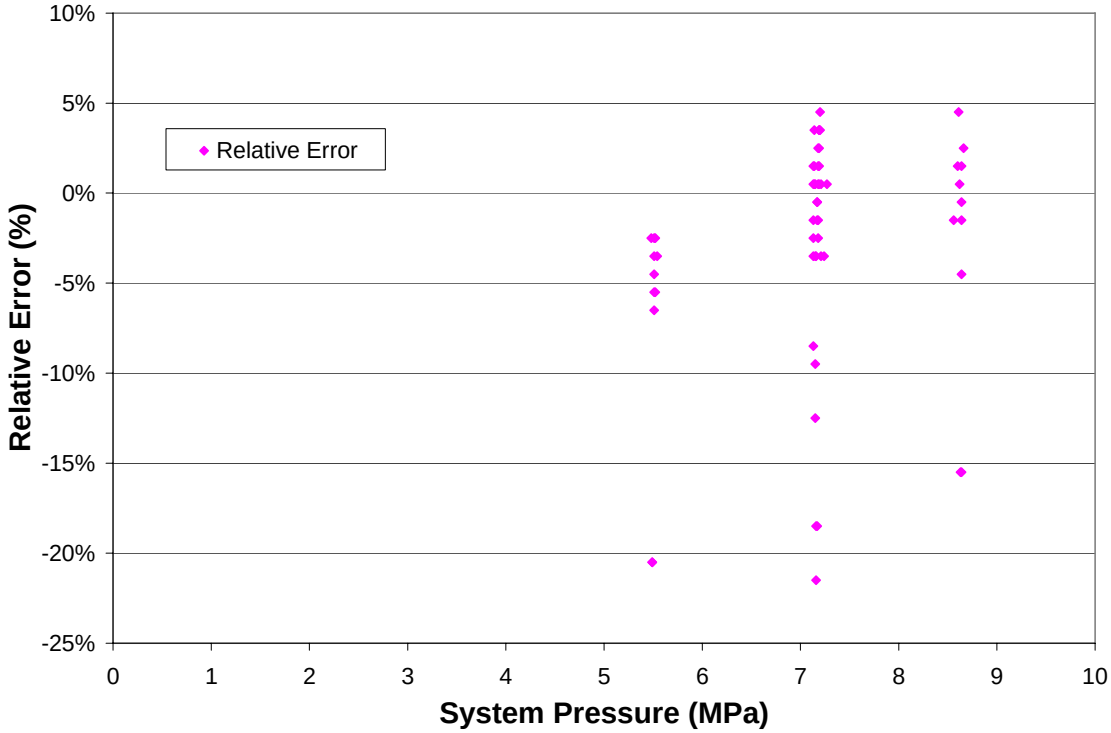

Figure 14. Effect of Pressure on CHF Prediction Accuracy

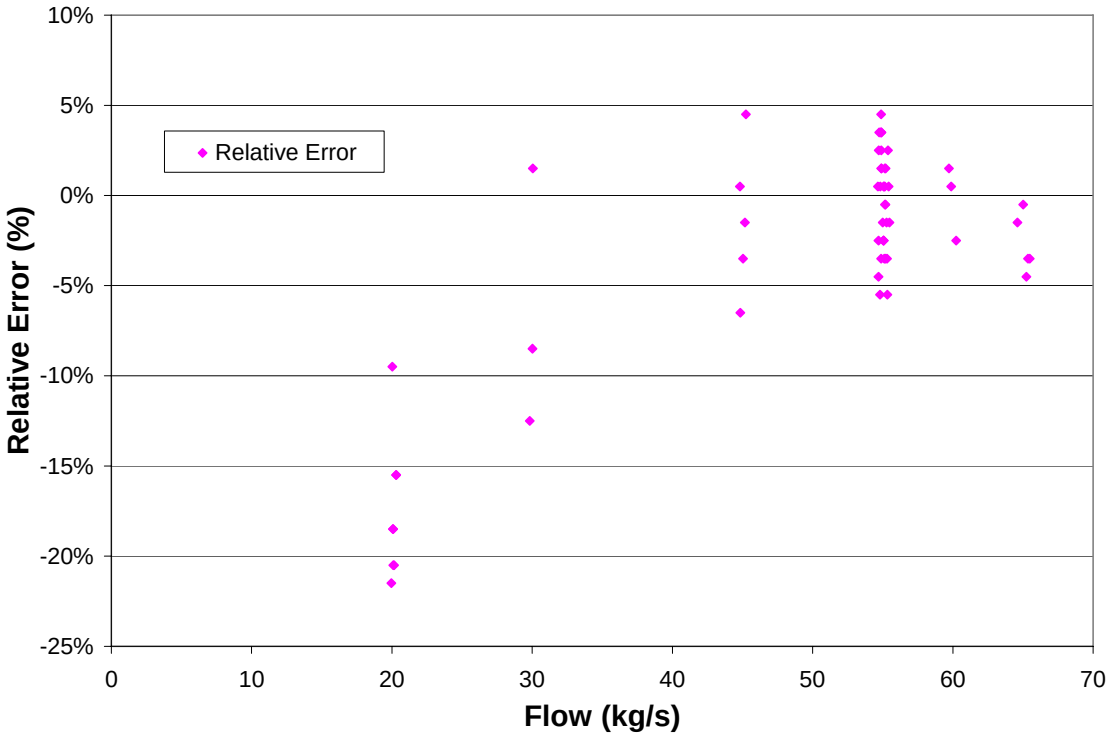

Figure 15. Effect of Flow on CHF Prediction Accuracy

b. Transient

As shown in Figures 16 and 17 (Configuration C3 turbine trip and pump trip, respectively), the COBRA-IE transient critical power calculations yielded temperature histories consistent with the measured data. Each data set in Figures 16 and 17 represents a temperature history from a different location on a rod where CHF occurs. In most cases, critical power was calculated to occur within 1 second of the measured time. In the measured data, all four thermocouple locations indicated CHF at approximately the same time, while in the COBRA-IE turbine trip results CHF was only indicated by one thermocouple location. This result indicates that the actual CHF was more widespread than the calculated CHF. Since CHF is calculated by COBRA-IE based on subchannel fluid properties and flow conditions, activation of the turbulent mixing and/or void drift models may allow for more mixing and improve calculational accuracy in transient simulations. Rewetting was reasonably simulated by the code in both cases, and results from Configuration C2A showed similar trends. COBRA-IE features several rewetting T_{min} model options that may be explored in the future; however, in the interest of baselining the code the default original COBRA-TF model was used in the calculations. Deficiencies in this relatively simple model may have contributed to the uncertainties seen in some of the results. It should also be noted that the primary focus of this analysis was the onset of transient CHF; therefore no attempt has been made to resolve the discrepancies seen with the rewetting phenomenon.

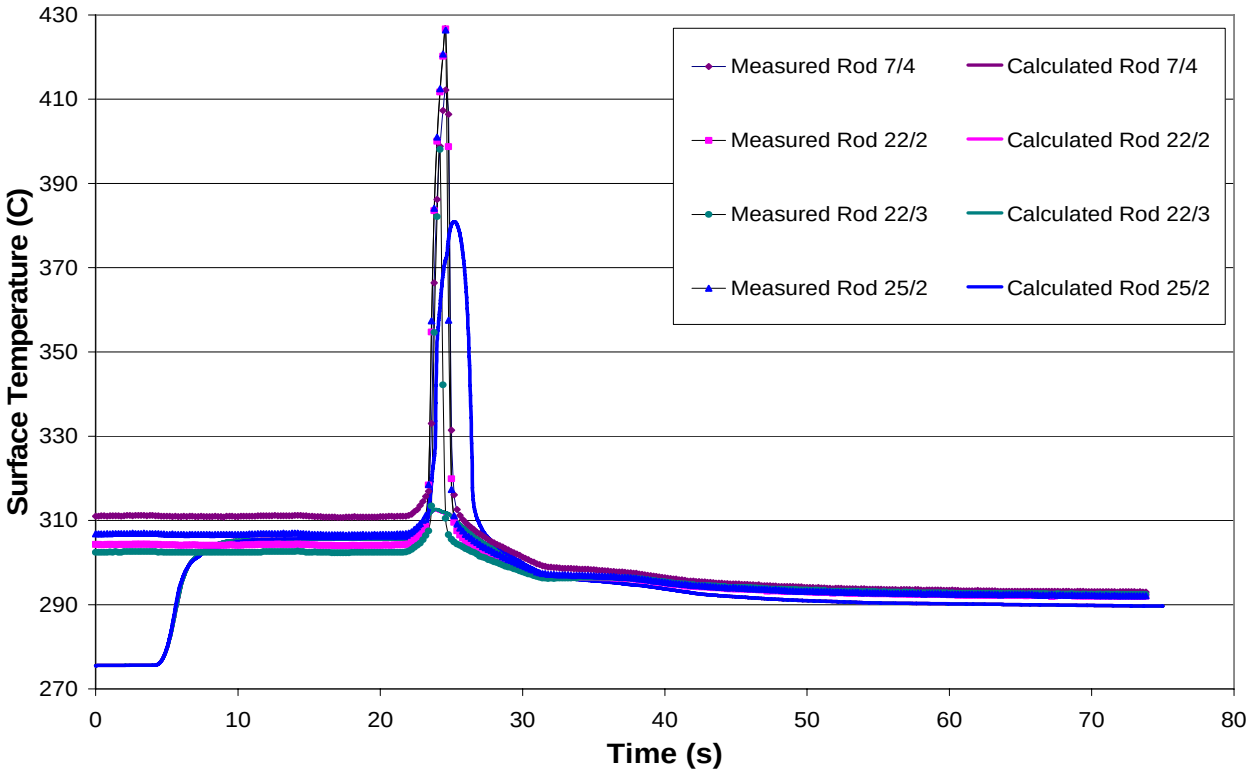

Figure 16. Turbine Trip Transient Critical Power Temperature Histories

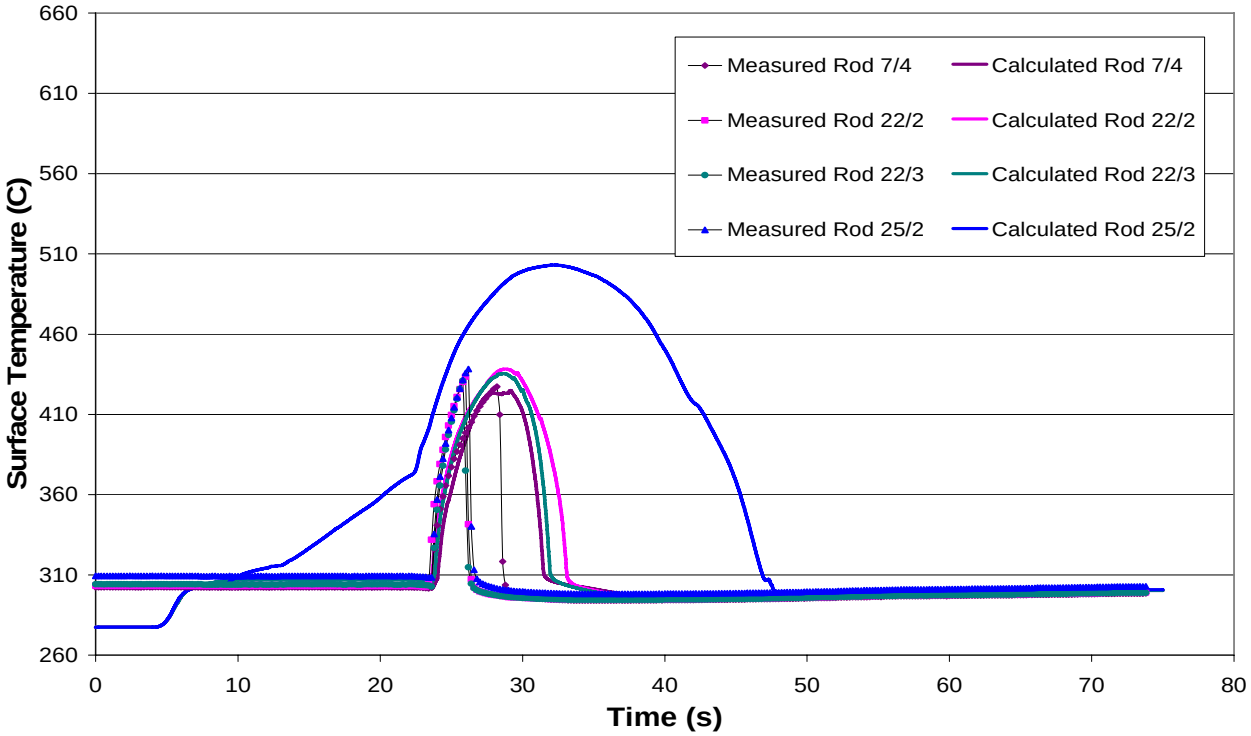

Figure 17. Pump Trip Transient Critical Power Temperature Histories

VII. Conclusion

From the COBRA-IE calculation results, it can be reasonably concluded that the code is capable of performing BWR subchannel analyses, including calculations of void distributions, pressure drop, and critical power. Void distributions were well-predicted for high exit quality ($\geq$12%) cases representative of BWR operating conditions. Pressure drop calculations proved accurate, with less than 1% average error in single-phase cases and 11% average error in two-phase cases. COBRA-IE performed well in critical power calculations as well, with 5% average error in the steady-state cases and the onset of CHF accurately captured in the transient cases.

As many of the optional models in COBRA-IE were disabled to provide an accurate baseline of the code's performance, sensitivity studies involving these models and their adjustable parameters should be performed in the future. Such studies may include investigating the impact of activating or modifying void drift, turbulent mixing, and T_{min} rewetting models, as well as testing additional CHF correlations.

Acknowledgements

The analysis and results presented here were performed under a U. S. Department of Energy contract with Bechtel Bettis, Inc.

References

1. Inoue, A. *et al*., 1995, "Void Fraction Distribution in BWR Fuel Assembly and Evaluation of Subchannel Code," *Journal of Nuclear Science and Technology*, 32, pp. 629-640.

2. Weaver, W. L., E. T. Tomlinson and D. L. Aumiller, 2002, “A PVM Executive Program for Use with RELAP5-3D,” *Proceedings of ICONE-10*, Arlington VA, April 2002.

3. Aumiller, D. L, E. T. Tomlinson, and R. C. Bauer., 2002. “Incorporation of COBRA-TF in an Integrated Code System With RELAP5-3D Using Semi-Implicit Coupling”, Available as B-T-3451 from DOE Office of Scientific and Technical Information.

4. Weaver, W. L., Tomlinson, E. T., Aumiller, D. L., 2001, “A Generic Semi-Implicit Coupling Methodology For Use In RELAP5-3D©,” *Nuclear Engineering and Design*, 211, pp. 13-26.

5. Holowach, M. J., “The Development of a Reflood Heat Transfer Computational Package for Small Hydraulic Diameter Geometries”, The Pennsylvania State University, Master of Science Thesis, 2000.

6. Todreas, N. E., and M. S. Kazimi. *Nuclear Systems I: Thermal Hydraulic Fundamentals*. Bristol, PA: Taylor & Francis, 1993.

7. Chun, T., Hwang, D., Baek, W. P., and S. H. Chang, 1998, "Assessment of a Tube-Based Bundle CHF Prediction Method Using a Subchannel Code," *Annals of Nuclear Energy*, 25, 1159-1168.